

Double layer capacitance and a microscopic structure of electrified liquid–liquid interfaces

L.I. Daikhin, M. Urbakh *

School of Chemistry, Tel Aviv University, 69978 Tel Aviv, Israel

Received 11 February 2003; received in revised form 16 June 2003; accepted 24 June 2003

Abstract

We develop a theory of the double layer at electrolyte–electrolyte interfaces taking in to account the microscopic structure of the interfacial region. This includes a “mixed boundary layer” where the overlapping of two space-charge regions occurs, and the effects of ion association and adsorption at the interface. Theoretical results are in good agreement with experimental data obtained for various organic solvents and electrolytes. The theory suggests a framework for the treatment of the capacitance data and establishes a relationship between experimental results and the microscopic structure of interfaces between two immiscible electrolyte solutions (ITIES).

© 2003 Elsevier B.V. All rights reserved.

Keywords: Liquid–liquid interfaces; Capacitance; Ion penetration; Ion pair interactions

1. Introduction

The electrochemical properties of interfaces between two immiscible electrolyte solutions (ITIES) have been actively investigated during the last 20 years [1–3]. These interfaces are formed between an organic solvent containing a hydrophobic salt and an aqueous electrolyte solution. Most information on ITIES has been obtained by classical electrochemical techniques including cyclic voltammetry and impedance measurements [1,2,4–6]. Thus one of the most basic experimental characteristics of the interface between two immiscible liquids is a double layer capacitance. Capacitance properties of ITIES are quite different from that extensively studied for metal–solution interfaces. In contrast to the metal–solution interfaces, it was found that the capacitance of ITIES depends strongly on the nature of the ions [2,6–11]. Often the capacitance curves show a strong asymmetry as a function of the potential and essential

deviations from the Gouy-Chapman behaviour even near the pzc. The discrepancy between experimental results and predictions of the Gouy-Chapman theory stimulated theoretical work, which went beyond the classical scheme [12,13] including the “mixed boundary layer”, ion adsorption and ion pairing at the interface [9–11,14–19]. It has been also shown that a thermally induced corrugation of liquid–liquid interfaces can strongly influence the capacitance dependence on the potential drop and on ionic strength [20–22]. However, in spite of numerous efforts, the structure of the ITIES is still a matter of controversy and there is no unambiguous picture for interpretation of capacitance data.

In this work we develop a mean-field theory of the double layer of ITIES, which takes into account effects of overlapping of the two space-charge regions, ion adsorption and ion association at the interface. The theory extends our recent studies [19], which have been focused on the effect of ion penetration into an “unfriendly medium” and described this effect within a perturbation approach. Here we overcome limitations of the perturbation approach that allows the treatment of experiments in which a measured capacitance differs essentially from the Gouy-Chapman prediction. We

*Corresponding author. Tel.: +972-3-640-8324; fax: +972-3-640-9293.

E-mail address: urbakh@post.tau.ac.il (M. Urbakh).

perform a detailed analysis of experimental data obtained for various solvents and electrolytes [23] and establish relationships between experimental results and a microscopic structure of ITIES.

2. Double layer theory

Consider a contact between two immiscible electrolyte solutions characterized by dielectric constants, ϵ_1 and ϵ_2 , and Debye lengths, κ_1^{-1} and κ_2^{-1} , respectively (see Fig. 1). For 1-1 binary electrolyte solutions $\kappa_i^{-1} = (\epsilon_i k_B T / 8\pi n_i^0 e^2)^{1/2}$, where n_i^0 is the bulk electrolyte concentration in the corresponding phase ($i = 1, 2$), e , the charge of proton, T , the temperature, and k_B , the Boltzmann constant. Here we assume that the ions that have affinity to one solution cannot penetrate into the bulk of the other solution, in other words the system “stays inside” the potential window over which the interface is ideally polarizable. Then the bulk of solvent 1 ($z \ll 0$), contains only anions and cations of sort 1, $\left(\begin{smallmatrix} \pm \\ 1 \end{smallmatrix}\right)$, while the bulk of solvent 2 ($z \gg 0$) contains ions of sort 2, $\left(\begin{smallmatrix} \pm \\ 2 \end{smallmatrix}\right)$. Here we also assume that the interface is flat and all properties of the system are functions of the distance from the interface, z , only.

2.1. Perturbation approach

Recently we have developed a theory of the double layer at ITIES [19], which takes into account the overlap of the two back-to-back double layers in the interfacial region and a smooth variation of dielectric properties across the interface. A solution of a modified nonlinear Poisson–Boltzmann equation has been obtained within the *perturbation theory*, which utilizes the smallness of

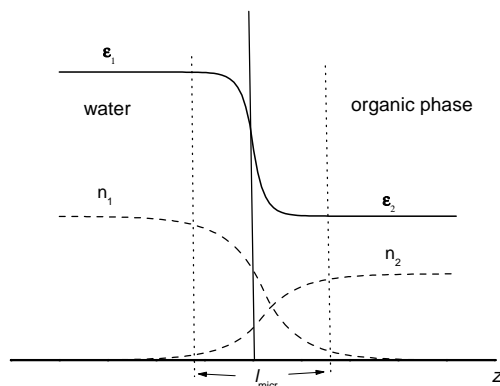


Fig. 1. An interface between two immiscible electrolyte solutions: dielectric constant profile, $\epsilon(z)$ (upper solid curve) and distributions of ionic concentrations, $n_i(z)$ (lower dashed curves), l_{micr} is the thickness of the microscopic interface layer.

the ratio of the “mixed layer” thickness to the Debye lengths in the adjacent solutions. It has been shown that the capacitance dependence on the nature of the ions is controlled by *three integral parameters*, L_1 , L_2 and L_3 which are expressed through the z -dependent energy profiles of ion transfer across the interface, $f_i^\pm(z)$, and through the dielectric profile of the solvent–solvent interface, $\epsilon(z)$ (see Fig. 1)

$$C = dQ/dE \\ = C_{\text{GC}}^0 \left[\frac{dU_0}{dV} + L_1 \frac{dU_1}{dV} + L_2 \frac{dU_2}{dV} + L_3 \frac{dU_3}{dV} \right]. \quad (1)$$

Here C_{GC}^0 is the Gouy-Chapman capacitance of the two back-to-back ionic double layers separated by a sharp interface at the point of zero charge [1,2]

$$C_{\text{GC}}^0 = \frac{\epsilon_1 \kappa_1 \epsilon_2 \kappa_2}{4\pi(\epsilon_1 \kappa_1 + \epsilon_2 \kappa_2)}, \quad (2)$$

$$L_1 = \int_{-\infty}^{+\infty} dz \left[\exp(-f_1^+(z)/k_B T) - \exp(-f_1^-(z)/k_B T) \right], \quad (3)$$

$$L_2 = \int_{-\infty}^{+\infty} dz \left[\exp(-f_2^+(z)/k_B T) - \exp(-f_2^-(z)/k_B T) \right], \quad (4)$$

$$L_3 = \int_{-\infty}^{+\infty} dz \left[\frac{1}{2} \left(\frac{1}{\epsilon_1} \exp(-f_1^+(z)/k_B T) + \frac{1}{\epsilon_1} \exp(-f_1^-(z)/k_B T) + \frac{1}{\epsilon_2} \exp(-f_2^+(z)/k_B T) + \frac{1}{\epsilon_2} \exp(-f_2^-(z)/k_B T) \right) - \frac{1}{\epsilon(z)} \right] \quad (5)$$

and $U_0(V)$, $U_1(V)$, $U_2(V)$ and $U_3(V)$ are the functions of the overall potential drop, E , and the bulk properties of the contacting electrolyte solutions (dielectric constants and ionic concentrations), $V = eE/k_B T$ is the dimensionless potential drop across the interface. The explicit equations for $U_0(V)$, $U_1(V)$, $U_2(V)$ and $U_3(V)$ are given in [19].

All three parameters L_1 , L_2 and L_3 are independent of the potential and ionic concentrations and have the dimensions of length. The absolute values of these lengths may be of the order of the thickness of a “mixed boundary layer” where the overlapping of the two space-charge regions occurs, but their sign may be positive or negative depending on the profiles of the integrands.

The result obtained within the perturbation theory can be applied when the three characteristic lengths L_1 , L_2 and L_3 are smaller than the Debye lengths in contacting media, $L_1, L_2, L_3 < \kappa_1^{-1}$. Under these conditions the deviations of the measured capacitance from the Gouy-Chapman result should be small. However, in

most experiments [1,2,4,6–8,13,23] this condition is not satisfied and the measured capacitance differs essentially from the Gouy-Chapman value. Experimental data also indicate that pair interactions between ions near the interface that have been ignored within the analytical theory [19] can contribute essentially to the capacitance [23].

2.2. Beyond the perturbation approach

In the present paper we generalize the theory [19] in order to overcome the limitations of the perturbation approach and to include three contributions to the double layer capacitance that go beyond the Gouy-Chapman description: (1) an overlap of the two back-to-back double layers in the interfacial regions, (2) ion association across the phase boundary, and (3) a variation of dielectric properties across the interface.

In order to solve the problem we separate the ensemble of ions into three subsystems: (1) ions located in the microscopic interfacial layer where overlap of double layers and ion association occur and, (2) and (3) ions located in the diffuse double layers and in the bulk solutions of the contacting phases. In the first region the ion distribution can differ essentially from that given by the Gouy-Chapman theory, while in regions 2 and 3 the Gouy-Chapman theory works well. The boundaries between the interfacial layer and regions 2 and 3 are denoted as $z = -l$ and $z = l$, correspondingly. This separation can be done when the thickness of the microscopic layer is smaller than the thickness of the diffuse double layers in two solutions. The latter assumption is well justified for not too concentrated solutions and not too high voltage drops across the interface [14–16,24,25]. Under these conditions the microscopic layer can be contracted to a plane separating the contacting phases. The surface concentrations of the ions at this plane are expressed in terms of ionic distributions $n_i^\pm(z)$

$$\Gamma_i^\pm = \int_{l_{\text{micr}}} dz n_i^\pm(z), \quad (6)$$

where l_{micr} is the thickness of the microscopic interfacial layer.

Density profiles of the ions, $n_i^\pm(z)$, and a distribution of electrostatic potential, $\phi(z)$, at the interface can be calculated using the functional of the free energy of two contacting electrolyte solutions. We start from a free energy functional that contains the contributions of the interfacial layer, F_S , and of the diffuse double layers and the bulk solutions, F_{GC}

$$F = F_S + F_{GC}. \quad (7)$$

The free energy F_{GC} consists of the electrostatic interaction and the entropy of diluted electrolytes [19]

$$\begin{aligned} F_{GC} = & -\frac{1}{8\pi} \int_{-\infty}^{-l} dz \varepsilon(z) [\nabla \phi(z)]^2 - \frac{1}{8\pi} \int_l^{\infty} dz \varepsilon(z) [\nabla \phi(z)]^2 \\ & + e \int_{-\infty}^{-l} dz \phi(z) (n_1^+(z) - n_1^-(z)) \\ & + e \int_l^{\infty} dz \phi(z) (n_2^+(z) - n_2^-(z)) \\ & - Ee \int_{-\infty}^{-l} (n_1^+(z) - n_1^-(z)) dz \\ & + k_B T \left[\int_{-\infty}^{-l} dz [n_1^+(z) \log(n_1^+(z)v_1) \right. \\ & \left. + n_1^-(z) \log(n_1^-(z)v_1) - (n_1^+(z) + n_1^-(z))] \right] \\ & + k_B T \left[\int_l^{\infty} dz [n_2^+(z) \log(n_2^+(z)v_2) \right. \\ & \left. + n_2^-(z) \log(n_2^-(z)v_2) - (n_2^+(z) + n_2^-(z))] \right]. \quad (8) \end{aligned}$$

The free energy of the interfacial layer, F_S , can be written as

$$\begin{aligned} F_S = & e(\Gamma_2^+ - \Gamma_2^-)\phi(0) + e(\Gamma_1^+ - \Gamma_1^-)(\phi(0) - E) \\ & + k_B T \sum_{i=1}^2 \left[\Gamma_i^+ \left(\ln \left(\frac{\Gamma_i^+}{\Gamma_{i0}^+} \right) - 1 \right) \right. \\ & \left. + \Gamma_i^- \left(\ln \left(\frac{\Gamma_i^-}{\Gamma_{i0}^-} \right) - 1 \right) \right] + k_B T \sum_{i=1}^2 [u_i^+ \Gamma_i^+ + u_i^- \Gamma_i^-] \\ & + k_B T [w_{12} \Gamma_2^+ \Gamma_1^- + w_{21} \Gamma_2^- \Gamma_1^+]. \quad (9) \end{aligned}$$

The first two terms in Eq. (9) describe the electrostatic contribution to F_S while the third term presents the entropy of ions at the interface. The last two terms take into account interactions of ions with the interface and short-range ion–ion interactions in the layer. The following notations have been used in Eqs. (8) and (9): v_i is the volume per molecule of the solvent (i), Γ_{i0} is the maximal value of surface excess for the ion of kind i which in general can be different for anions and cations, u_i^\pm is a constant of interaction (in units of $k_B T$) between the ion and the interface which represents the effects of ion adsorption and penetration across the interface, parameters $w_{12(21)}$ describe the short-range interaction of an anion from phase 1 (2) with a cation from phase 2 (1). More precisely $w_{12(21)}$ present the ensemble-averaged energy of ion–ion interaction multiplied by the area πa^2 where a is the radius of action of the ion–ion potential. In order to obtain $w_{12(21)}$ from the results of molecular dynamics simulation the averaging over different orientations and locations of ionic pairs with respect to the interface should be performed.

The expression for the free energy (7) does not include the effect of saturation in the microscopic interfacial region. This effect can be important for high electrolyte

concentrations, large ions or ionic absorption. In these cases the following terms should be added to Eq. (9)

$$k_B T \sum_{i=1}^2 \left[(\Gamma_{i0} - \Gamma_i^+) \left(\ln \left(\frac{\Gamma_{i0} - \Gamma_i^+}{\Gamma_{i0}} \right) - 1 \right) + (\Gamma_{i0} - \Gamma_i^-) \left(\ln \left(\frac{\Gamma_{i0} - \Gamma_i^-}{\Gamma_{i0}} \right) - 1 \right) \right]. \quad (10)$$

The effect of saturation will be considered elsewhere.

In order to derive equations for the electrostatic potential, the ionic concentrations and the surface concentrations we minimize the grand potential, Ω

$$\Omega = F - \mu_1 \int_{-\infty}^{-l} dz [n_1^+(z) + n_1^-(z)] - \mu_2 \int_l^{\infty} dz [n_2^+(z) + n_2^-(z)] - \sum_{i=1}^2 \mu_i [\Gamma_i^+ + \Gamma_i^-] \quad (11)$$

with respect to ϕ , n_i^\pm and Γ_i^\pm . Here μ_i is the chemical potential of positive and negative ions of kind i which is related to the bulk concentration of the corresponding electrolyte through the relation

$$\mu_i = k_B T \ln(n_i^0 v_i). \quad (12)$$

In this way we obtain:

(1) the Poisson–Boltzmann equation for the electrostatic potential

$$\frac{d}{dz} \varepsilon(z) \frac{d}{dz} \psi(z) = - \frac{4\pi e^2}{k_B T} N[\psi(z)] - \sigma \delta(z), \quad (13)$$

where $N[\psi(z)] = [n_1^+(z) - n_1^-(z)]\theta(-l-z) + [n_2^+(z) - n_2^-(z)]\theta(z-l)$ is the charge density in the diffuse layers and $\sigma = 4\pi e^2/k_B T \sum_{i=1}^2 [\Gamma_i^+ - \Gamma_i^-]$ is the surface charge density, $\psi = e\phi/k_B T$;

(2) the relationships between the ionic concentrations and the potential in the diffuse layers

$$n_1^\pm(z) = n_{10} \exp[\mp(\psi(z) - V)], \quad (14)$$

$$n_2^\pm(z) = n_{20} \exp[\mp\psi(z)] \quad (15)$$

(3) and the equations for the determination of the surface concentrations of ions

$$\Gamma_1^+ = n_{10} v_1 \Gamma_{10} \exp [(-\psi(0) + V) - u_1^+ - w_{21} \Gamma_2^-], \quad (16)$$

$$\Gamma_1^- = n_{10} v_1 \Gamma_{10} \exp [(\psi(0) - V) - u_1^- - w_{12} \Gamma_2^+], \quad (17)$$

$$\Gamma_2^+ = n_{20} v_2 \Gamma_{20} \exp [-\psi(0) - u_2^+ - w_{12} \Gamma_1^-], \quad (18)$$

$$\Gamma_2^- = n_{20} v_2 \Gamma_{20} \exp [\psi(0) - u_2^- - w_{21} \Gamma_1^+]. \quad (19)$$

The quantities, $\Gamma_{i0} v_i$, in Eqs. (16)–(19) have the dimension of length and are usually named as adsorption lengths, $l_{a,i} \equiv \Gamma_{i0} v_i$.

2.3. Calculation of the capacitance

First we solve Eqs. (13)–(19) assuming a sharp variation of the dielectric function across the interface,

$\varepsilon(z) = \varepsilon_0(z) = \varepsilon_1 \theta(-z) + \varepsilon_2 \theta(z)$. Later a smearing of the dielectric profile will be taken into account within the perturbation approach discussed in [19].

The distribution of the electrostatic potential can be obtained from Poisson's equation (13), which includes both the bulk (diffuse layer) and surface charge densities. In order to perform calculations in the spirit of Gouy–Chapman theory it is convenient to rewrite the bulk and surface terms in the rhs of Eq. (13) in the following form

$$N[\psi(z)] \rightarrow N[\psi(z)] = [n_1^+(z) - n_1^-(z)]\theta(-z) + [n_2^+(z) - n_2^-(z)]\theta(z), \quad (20)$$

$$\sigma \rightarrow \sigma = \frac{4\pi e^2}{k_B T} [(\Gamma_1^+ - \ln_1^+(0)) - (\Gamma_1^- - \ln_1^-(0)) + (\Gamma_2^+ - \ln_2^+(0)) - (\Gamma_2^- - \ln_2^-(0))]. \quad (21)$$

Here we extended the ranges of the diffuse layers up to the interface, $z = 0$, and in order to keep the total charge density, $N[\psi(z)] + \sigma$, unchanged we subtracted the terms added to $N[\psi(z)]$ from the surface contribution, σ . Then the solution of Eq. (13) gives

$$\psi(z) = V - 4 \arctan[\exp(\kappa_1(z + z_{10}))] \quad \text{for } z \leq 0, \quad (22)$$

$$\psi(z) = 4 \arctan[\exp(-\kappa_2(z + z_{20}))] \quad \text{for } z > 0, \quad (23)$$

where z_{10} and z_{20}

$$z_{10} = -2\kappa_1^{-1} \arctan \left\{ \left(\sigma + \sqrt{\sigma^2 + 4(\varepsilon_2 \kappa_2 + \varepsilon_1 \kappa_1 e^{V/2})(\varepsilon_2 \kappa_2 + \varepsilon_1 \kappa_1 e^{-V/2})} \right) / 2(\varepsilon_2 \kappa_2 e^{V/2} + \varepsilon_1 \kappa_1) \right\}, \quad (24)$$

$$z_{20} = 2\kappa_2^{-1} \arctan \left\{ \left(-\sigma + \sqrt{\sigma^2 + 4(\varepsilon_2 \kappa_2 + \varepsilon_1 \kappa_1 e^{V/2})(\varepsilon_2 \kappa_2 + \varepsilon_1 \kappa_1 e^{-V/2})} \right) / 2(\varepsilon_2 \kappa_2 + \varepsilon_1 \kappa_1 e^{V/2}) \right\}. \quad (25)$$

It should be noted that the surface charge density, σ , entering Eqs. (24) and (25) is not an independent variable, but is a function of the potential at the interface, $\psi(0)$. A relation between σ and $\psi(0)$ obtained from Eqs. (22)–(25) reads

$$(\varepsilon_2 \kappa_2 + \varepsilon_1 \kappa_1 e^{V/2}) \exp(-\psi(0)) + \sigma \exp(-\psi(0)/2) = (\varepsilon_2 \kappa_2 + \varepsilon_1 \kappa_1 e^{-V/2}). \quad (26)$$

Eqs. (14)–(19), (21) and (26) present a complete system that allows the double layer capacitance, surface charge densities and potential distribution to be determined.

The net result for the double layer capacitance is finally given by

$$C = \frac{C_d^{(1)} C_d^{(2)}}{C_d^{(1)} + C_d^{(2)}} \left\{ 1 + \frac{e}{C_d^{(1)}} \left[\frac{d\Gamma_1^+}{dE} - \frac{d\Gamma_1^-}{dE} \right] - \frac{e}{C_d^{(2)}} \left[\frac{d\Gamma_2^+}{dE} - \frac{d\Gamma_2^-}{dE} \right] \right\}, \quad (27)$$

where $C_d^{(1)}$ and $C_d^{(2)}$ are the diffuse double layer capacitances in the contacting phases 1 and 2, which are calculated within the Gouy-Chapman theory considering the surface charge density in addition to the charge in the diffuse double layer

$$C_d^{(1)} = \frac{\varepsilon_1 \kappa_1}{4\pi} \cosh \left[\frac{\psi(0) - V}{2} \right], \quad (28)$$

$$C_d^{(2)} = \frac{\varepsilon_2 \kappa_2}{4\pi} \cosh \left[\frac{\psi(0)}{2} \right]. \quad (29)$$

Eq. (27) shows a general resemblance to the equations for the double layer capacitance derived in [9,23]. Contrary to the previous work [9,23] where ionic association was considered in terms of ion-pair equilibrium, here we take into account explicitly the dependence of surface ion concentration on the potential and include all ion–interface and ion–ion interactions. Therefore the predictions of our model differ from the results of [9,23]. It should be noted that under the conditions, $\Gamma_1^+ = \Gamma_2^+$; $\Gamma_1^- = \Gamma_2^-$ and

$$\frac{d\Gamma_1^+}{dE} = \frac{e}{k_B T} \Gamma_1^+, \quad \frac{d\Gamma_1^-}{dE} = -\frac{e}{k_B T} \Gamma_1^-,$$

Eq. (27) for the capacitance reduces to that derived in [9]. However, our calculations show that the latter conditions do not hold for realistic values of the system parameters.

Below we demonstrate that a comparison of our theoretical results with experimental data allows us to determine the interaction constants, u_i^\pm and $w_{12(21)}$, in-

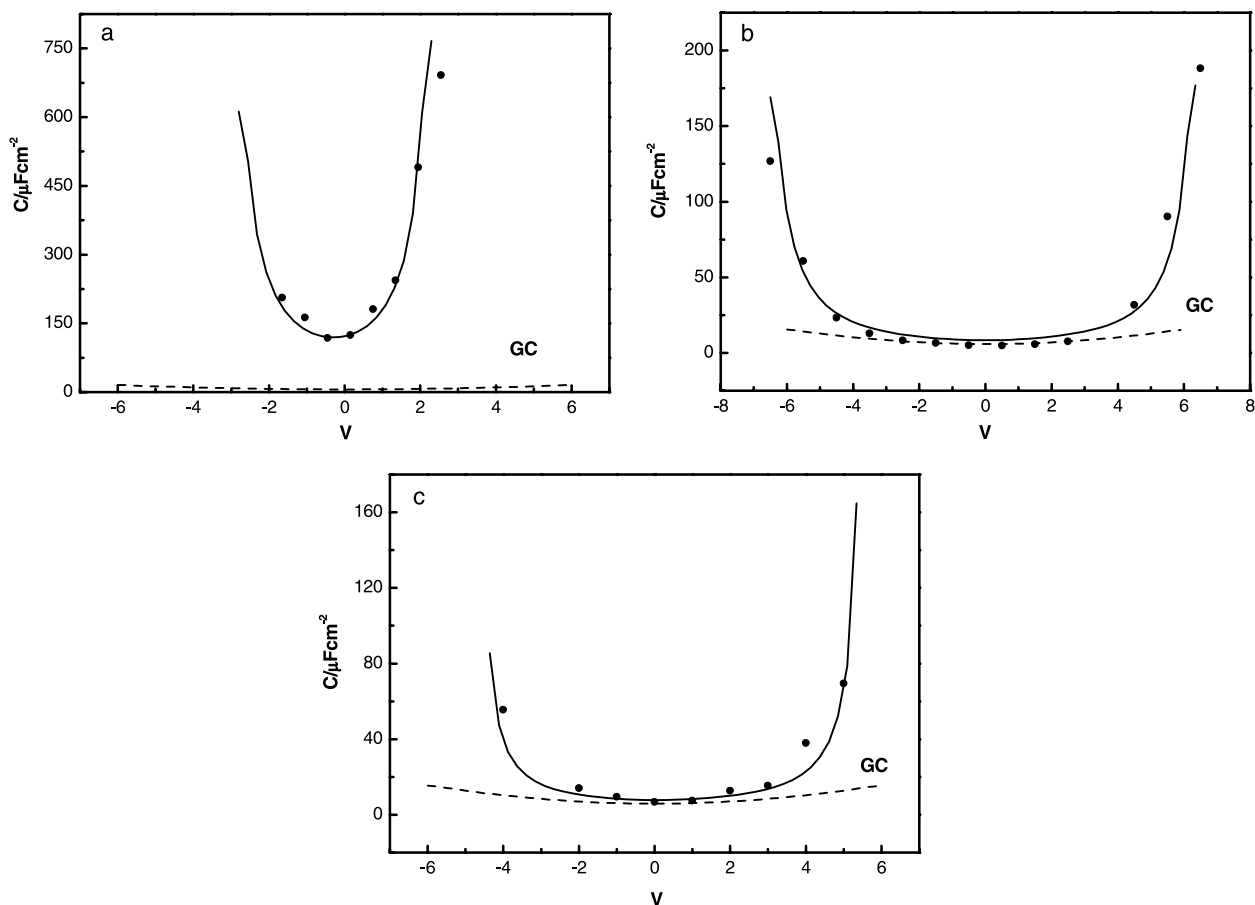


Fig. 2. Capacitance–dimensionless potential curves with 2-heptanone as the organic solvent. Aqueous phase contains 10 mM LiCl; the organic phase contains 10 mM: (a) TBATPB; (b) THATPB; (c) TOATPB. The experimental results are shown by dots, the dashed line represents the Gouy-Chapman result and the solid lines represents the theoretical curves calculated according Eqs. (27) and (32). Parameter values: (a) $u_1^+ = u_2^- = -5.7$; $u_2^+ = u_1^- = -5.4$; $w_{12}^* = -0.5$; $w_{21}^* = -0.5$; $L_e = -0.55$ Å. (b) $u_1^+ = u_2^- = -2.5$; $u_2^+ = u_1^- = -2.5$; $w_{12}^* = -1.3$; $w_{21}^* = -1.45$; $L_e = -0.55$ Å. (c) $u_1^+ = u_2^- = -2.35$; $u_2^+ = u_1^- = -2.35$; $w_{12}^* = -4.5$; $w_{21}^* = -2.8$; $L_e = -0.55$ Å, where $w_{12}^* = w_{12}\Gamma_{10}$ and $w_{21}^* = w_{21}\Gamma_{20}$. In all calculations we assumed $\Gamma_{10} = \Gamma_{20}$ and $l_{a,1} = l_{a,2} = l = 1$ Å.

volved in the model, and to understand the dependences of the double layer capacitance on the nature of the ions. It should be noted that all interaction constants can be calculated within the framework of molecular dynamics simulations. Thus this mean-field type model can provide a bridge between the “microscopic” description and experimental studies of ITIES.

In the absence of ion–ion interactions the system of Eqs. (14)–(19) and (26) can be solved analytically. Then for the case of a small effect of the interfacial layer on the capacitance, Eq. (27) for the capacitance takes the form of Eq. (1) which has been derived previously within the perturbation approach [19]. A comparison between Eqs. (1) and (27) allows us to establish the relationships between the parameters of ion–interface interaction, u_i^\pm , and the free energy profile functions for ion transfer across the interface, f_i^\pm

$$l_{a,1} \exp(-u_1^\pm) - l = \int_{-\infty}^{\infty} dz [\exp(-f_1^\pm(z)) - \theta(-z)], \quad (30)$$

$$l_{a,2} \exp(-u_2^\pm) - l = \int_{-\infty}^{\infty} dz [\exp(-f_2^\pm(z)) - \theta(z)]. \quad (31)$$

Eqs. (30) and (31) clarify the physical meaning of the interaction constants, u_i^\pm , introduced in this paper and allow us to calculate them from microscopic models of ITIES [17,18,25]. It should be noted that Eq. (27) for the capacitance has been derived within a model considering ion penetration into an “unfriendly medium”. Our calculations show that the same equation can be used for any type of interaction between ions and the interface. Particular features of this interaction affect the shape of the free energy profile functions, f_i^\pm and values of the interaction constants, u_i^\pm .

In a general case Eqs. (14)–(19), (21) and (26) should be solved numerically. Below we present results of such calculations, discuss the dependence of the double layer capacitance on the strength of ion–interface and ion–ion interactions and compare our theoretical results with the experimental data [23].

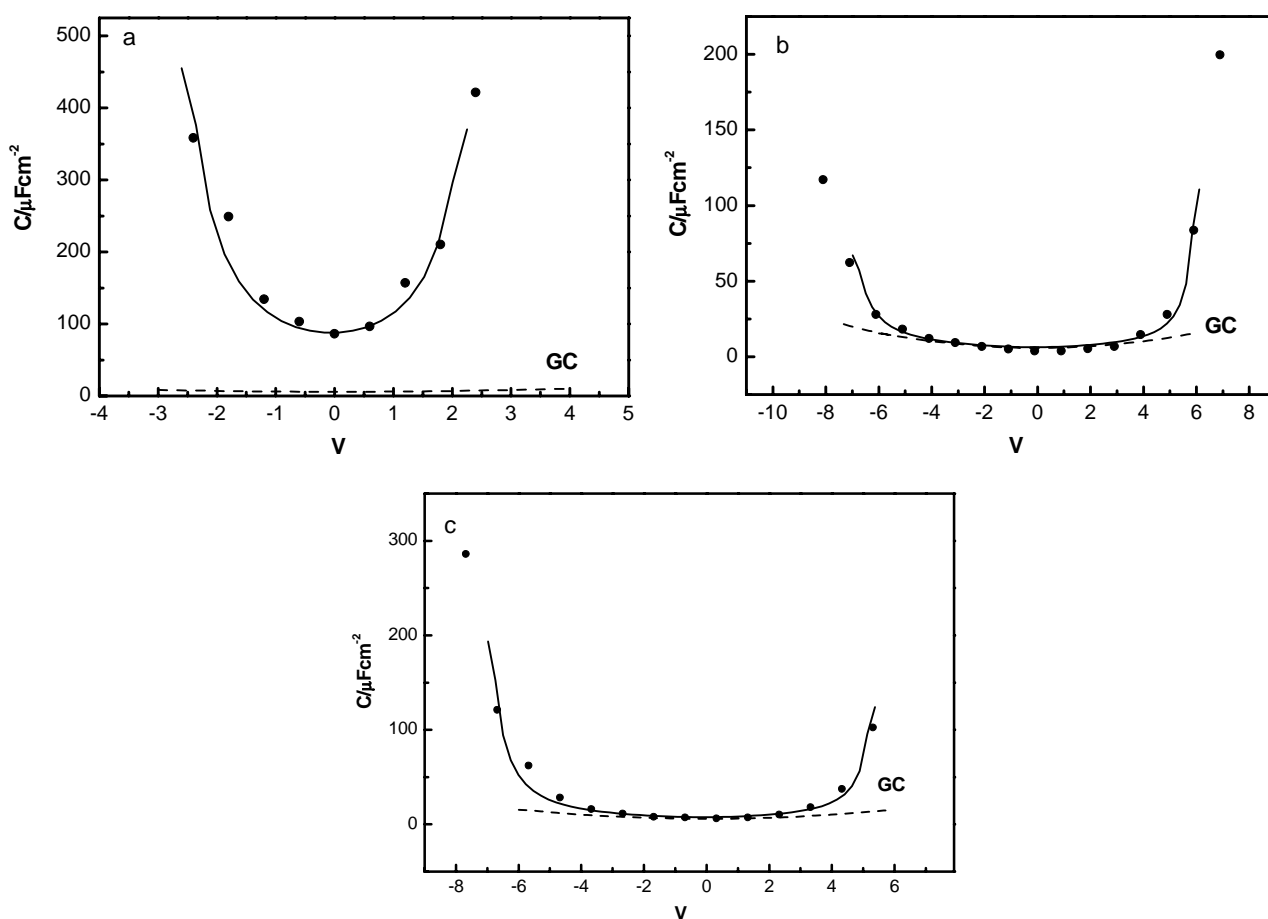


Fig. 3. As in Fig. 2, but with 2-octanone. Parameter values: (a) TBATPB: $u_1^+ = u_2^- = -5.2$; $u_2^+ = u_1^- = -5.2$; $w_{12}^* = -0.6$; $w_{12}^* = -0.7$; $L_\epsilon = -0.3 \text{ \AA}$. (b) THATPB: $u_1^+ = u_2^- = -1.6$; $u_2^+ = u_1^- = -1.5$; $w_{12}^* = -2.2$; $w_{21}^* = -3.8$; $L_\epsilon = -0.3 \text{ \AA}$. (c) TOATPB: $u_1^+ = u_2^- = -2.1$; $u_2^+ = u_1^- = -2.0$; $w_{12}^* = -1.6$; $w_{21}^* = -3.4$; $L_\epsilon = -0.3 \text{ \AA}$.

2.4. Comparison with the experimental data

Here we focus on the interpretation of capacitance measurements at the polarisable aqueous–organic interfaces, which have been performed varying both the solvent and the electrolyte of the organic phase [23]. The organic solvents used in these measurements were 1,2-dichloroethane, 2-heptanone, 2-octanone and 1,3-dibromopropane, while tetraphenylborates of tetraoctylammonium (TOATPB), tetrahexylammonium (THATPB), tetrabutylammonium (TBATPB), tetrapropylammonium (TPrATPB) and myristyltrimethylammonium (MTMATPB) were used as supporting electrolytes in the organic phase (see Figs. 2–5). It was found that experimental results depend strongly on the type of organic solvent and on the electrolyte [23]. It should be noted that in [19] the potential dependence of the capacitance has been extracted from the impedance data using the Randles scheme. Recent considerations [26] suggested that the fitting of impedance data to the Randles-type equivalent circuit can lead to an overestimation of the capacitance. Here we perform a compar-

ison of our theoretical results with the experimental data assuming an applicability of the Randles scheme. However, additional careful experimental studies are needed to establish a range of potentials where the Randles scheme can be applied.

The analysis of experimental data [23] within the theory developed here suggests that, based on the potential dependence of the capacitance the systems investigated can be separated into three main groups. The systems which fall in the first group (TBATPB in 2-heptanone and TBATPB in 2-octanone) show high values of the double layer capacitance at the pzc, followed by a steep rise of the capacitance even in the range of moderate potentials (see Figs. 2a and 3a). This behavior can be explained by assuming a strong interaction of ions with the interface, $|u_i^\pm| \gg 1$. According to Eqs. (30) and (31) large values of u_i^\pm point to a strong penetration of the corresponding ions across the interface (overlapping of the two-space-charge regions). It should be noted that the experimental observations for TBATPB in 2-heptanone and 2-octanone could be explained without considering the effects of pair interactions between anions and ca-

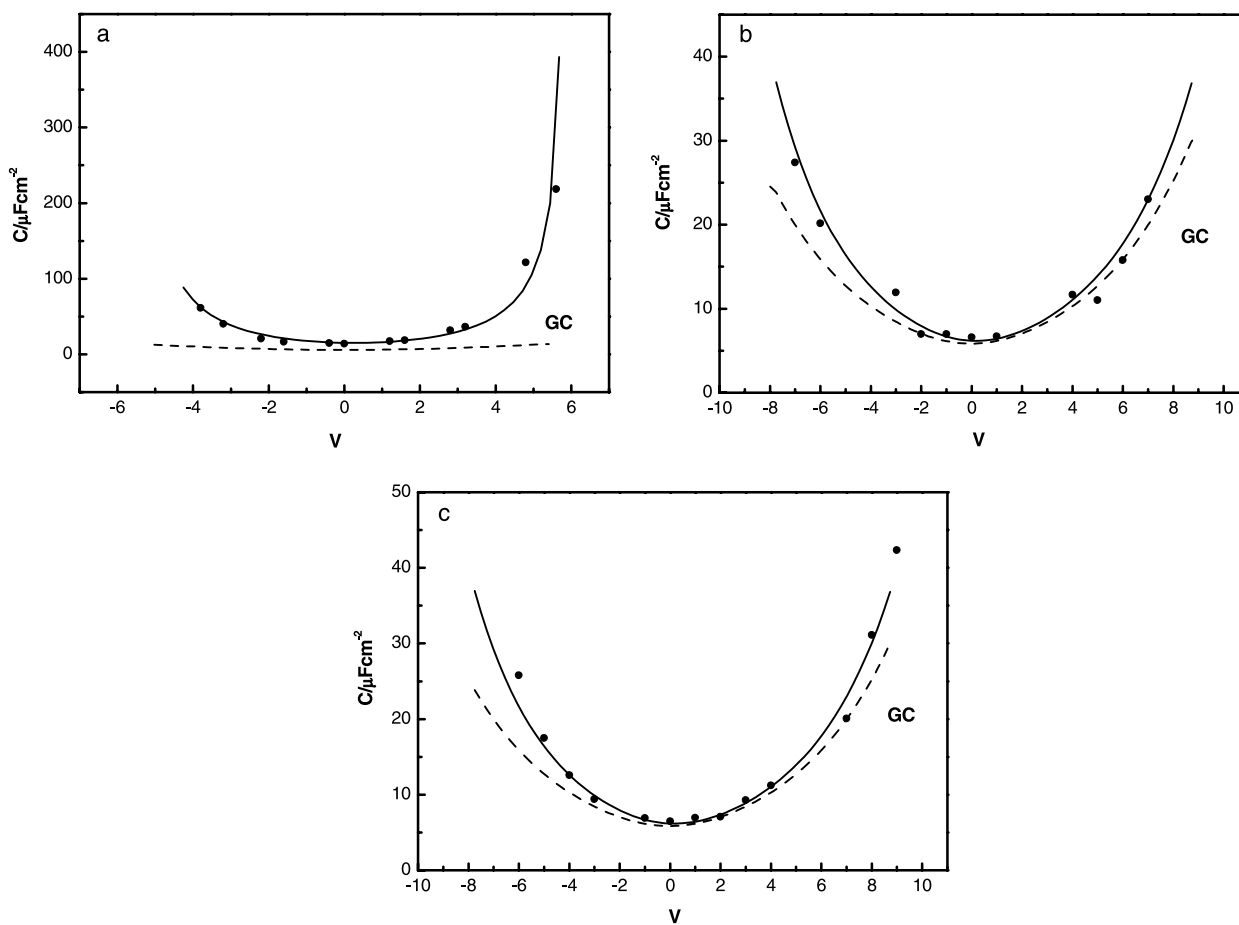


Fig. 4. As in Fig. 2, but with 1,3-dibromopropane. Parameter values: (a) TBATPB: $u_1^+ = u_2^- = -3.0$; $u_2^+ = u_1^- = -3.3$; $w_{12}^* = -1.5$; $w_{12}^* = -1.6$, $L_e = 0$. (b) THATPB: $u_1^+ = u_2^- = -0.3$; $u_2^+ = u_1^- = -0.8$; $w_{12}^* = 0$; $w_{21}^* = 0$, $L_e = 0$. (c) TOATPB: $u_1^+ = u_2^- = -0.3$; $u_2^+ = u_1^- = -0.8$; $w_{12}^* = 0$; $w_{21}^* = 0$, $L_e = 0$.

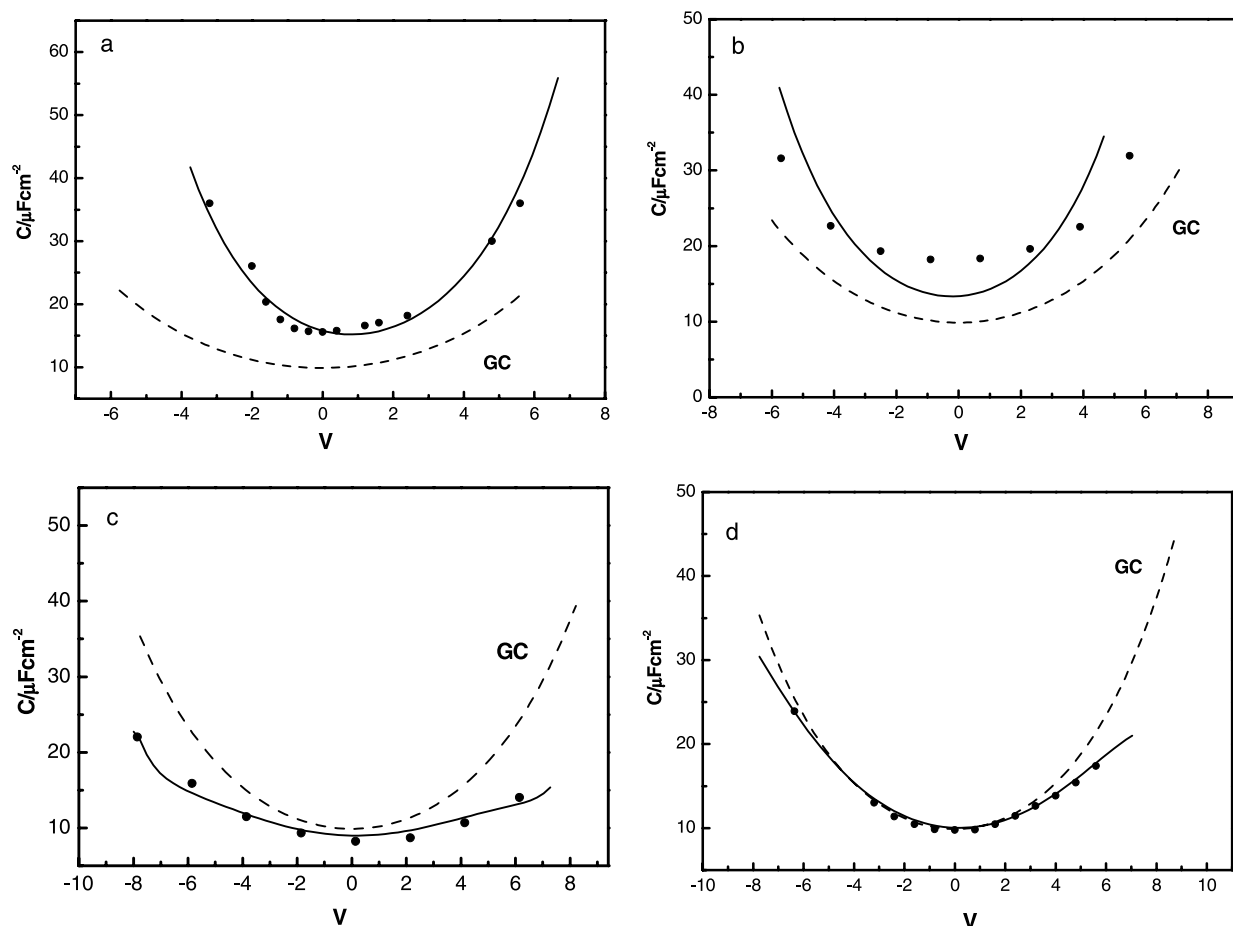


Fig. 5. Capacitance–dimensionless potential curves with 1,2-dichloroethane as the organic solvent. Aqueous phase contains 10 mM LiCl; the organic phase contains 50 mM: (a) TPrATPB; (b) MTMATPB; (c) TOATPB; (d) TBATPB. The experimental results are shown by dots, the dashed line represents Gouy-Chapman result and the solid lines represent the curves calculated according Eqs. (27) and (32). Parameter values: (a) $u_1^+ = u_2^- = -1.8$; $u_2^+ = u_1^- = -2.6$; $w_{12}^* = 0$; $w_{21}^* = 0$; $L_e = -0.2$ Å. (b) $u_1^+ = u_2^- = -2.$; $u_2^+ = u_1^- = -1.8$; $w_{12}^* = 0$; $w_{21}^* = 0$; $L_e = -0.2$ Å. (c) $u_1^+ = u_2^- = -0.7$; $u_2^+ = u_1^- = -0.8$; $w_{12}^* = -0.8$; $w_{21}^* = -1$; $L_e = -0.2$ Å. (d) $u_1^+ = u_2^- = -1.06$; $u_2^+ = u_1^- = -1.2$; $w_{12}^* = 0$; $w_{21}^* = 0$; $L_e = -0.2$ Å. The notations are the same as in Fig. 2.

tions. Figs. 2a and 3a demonstrate that for this choice of parameters, the theoretical results fit well the experimental data for TBATB in 2-heptanone and 2-octanone.

Handling the experimental data, we have also included the effect of smearing of the dielectric function near the interface. According to our previous results [19] this effect leads to an additional contribution to the capacitance in Eq. (27) which reads as

$$C_e = C_{GC}^0 L_e \frac{dU_3}{dV}, \quad (32)$$

where

$$L_e = \int_{-\infty}^{+\infty} dz \left[\frac{1}{\varepsilon_1} \theta(-z) + \frac{1}{\varepsilon_2} \theta(z) - \frac{1}{\varepsilon(z)} \right] \quad (33)$$

and the explicit equation for U_3 is given in [19]. Our calculations show that this contribution to the capacitance is essential for describing the experimental results

for TOATPB and TABATPB in 1,2-dichloroethane, where the measured capacitance is smaller than the Gouy-Chapman capacitance. In other systems the effect of smearing of the dielectric function does not play an essential role.

The second group of data (TOATPB and THATPB in 2-heptanone and 2-octanone, and TBATPB in 1,3-dibromopropane) is characterized by a capacitance, which is only slightly higher than the Gouy-Chapman value at the pzc, grows slowly with a potential in the range of moderate potentials ($|E| \leq 50$ – 100 mV), and increases steeply for higher potentials. These observations can be attributed to a small penetration of ions across the interface ($|u_i^\pm| \leq 1$), and a strong ion–ion interaction (ion association) at the interface (see Figs. 2b,c, 3b,c and 4a). Our calculations show that for modest values of the ion–surface interaction constants, $|u_i^\pm| \leq 1$, the effect of ion association comes into play at high potentials only. In this case there is only a marginal

effect of pair interactions on the capacitance at moderate potentials because of the smallness of the ion concentration at the interface under these conditions.

The potential dependences of the capacitance for TPrATPB and MTMATPB in 1,2-dichloroethane are intermediate between those for groups 1 and 2. We expect that here both ion penetration and association play some role, but these effects are less pronounced than for the systems discussed above (see Figs. 5a and b).

In the systems belonging to the third group (TOATPB and TBATPB in 1,2-dichloroethane, and THATPB and TOATPB in 1,3-dibromopropane) the potential dependence of the capacitance is similar to the Gouy-Chapman value (see Figs. 4b,c and 5c,d). This behavior points to a minor importance of ion penetration and association in the above-listed systems. The modest lowering of the observed capacitance compared to the Gouy-Chapman predictions, which was observed for TOATPB and TBATPB in 1,2-dichloroethane has been explained by taking into account the effect of smearing of the dielectric function near the interface. Figs. 5c and d show a good agreement between the results of our calculations and experimental data for TBATPB and TOATPB in 1,2-dichloroethane.

3. Conclusions

We have developed a theory of the double layer at electrolyte–electrolyte interfaces with account for a microscopic structure of the interfacial region. This includes a “mixed boundary layer” where the overlap of two space-charge regions occurs and effects of ion association and adsorption at the interface. The results obtained suggest a new framework for the treatment of the capacitance data and establish a relationship between the experimental results and the microscopic structure of ITIES. Comparison of the theoretical results with the experimental data [23] demonstrates that in accordance with the strength of ion–interface and ion–ion interactions, the systems investigated can be separated into three main groups. Fitting experimental data to Eqs. (27)–(29) one may evaluate the interaction constants, u_i^\pm and $w_{12(21)}^*$ which characterize ion–interface and ion–ion interactions at the interface and establish dependences of these parameters on the type of ion. We have found that a good agreement between the theory and experiment can be reached for the values of parameters u_i^\pm and $w_{12(21)}^*$ lying within the intervals $-5.7 \leq u_i^\pm \leq -0.3$, $-4.5 \leq w_{12(21)}^* \leq 0$. Here parameters u_i^\pm describe an energy of interaction between the ion $\left(\begin{smallmatrix} \pm \\ i \end{smallmatrix}\right)$ and the interface while the parameters $w_{12(21)}^* = w_{12(21)}\Gamma_{10(20)}$ present the ensemble averaged energy of pair interaction between an anion (cation) from phase 1 and a cation (anion) from phase 2 multiplied by the

number of nearest neighbors. It should be noted that the interaction constants, u_i^\pm and $w_{12(21)}^*$ can be calculated within molecular dynamics simulations [25,27]. Unfortunately so far the corresponding calculations have not been performed for the ions discussed in the paper. However, the interaction constants used in this work are in agreement with the parameters found for other ions [27] and used in previous model calculations [17,18].

Acknowledgements

Financial support of this work by the Israel Science Foundation (Grant No. 573/00) is gratefully acknowledged. We would like to thank Carlos M. Pereira for useful discussions.

References

- [1] H.H. Girault, D.H. Schiffrin, in: A.J. Bard (Ed.), *Electroanalytical Chemistry*, vol. 15, Marcel Dekker, New York, 1989, p. 1.
- [2] H.H. Girault, in: J.O'M. Bockris et al. (Eds.), *Modern Aspects of Electrochemistry*, vol. 25, Plenum Press, New York, 1993, p. 1.
- [3] A.G. Volkov, D.W. Deamer, D.I. Tanelian, V.S. Markin, *Liquid Interfaces in Chemistry and Biology*, Wiley, New York, 1998.
- [4] Z. Samec, *Chem. Rev.* 88 (1988) 617.
- [5] T. Kakiuchi, M. Senda, *Bull. Chem. Soc. Jpn.* 56 (1983) 1753.
- [6] C.M. Pereira, A. Martins, M. Rochas, A.J. Silva, A.F. Silva, *J. Chem. Soc., Faraday Trans.* 90 (1994) 143.
- [7] H.H. Girault, D.J. Schiffrin, *J. Electroanal. Chem.* 150 (1983) 43.
- [8] D. Homolka, P. Hajkova, V. Marecek, Z. Samec, *J. Electroanal. Chem.* 159 (1983) 233.
- [9] Y. Cheng, V.J. Cunnane, D.J. Schiffrin, L. Murtomaki, K. Kontturi, *J. Chem. Soc., Faraday Trans.* 87 (1991) 107.
- [10] C.M. Pereira, W. Schmickler, F. Silva, M.J. Sousa, *Chem. Phys. Lett.* 268 (1997) 13.
- [11] C.M. Pereira, W. Schmickler, F. Silva, M.J. Sousa, *J. Electroanal. Chem.* 436 (1997) 9.
- [12] E.J. Verwey, K.F. Niessen, *Philos. Mag.* 28 (1939) 435.
- [13] C. Gavach, P. Seta, B. d'Epenoux, *J. Electroanal. Chem.* 83 (1977) 225.
- [14] Z. Samec, V. Marecek, D. Homolka, *J. Electroanal. Chem.* 187 (1985) 31.
- [15] G.M. Torrie, J.P. Valteau, *J. Electroanal. Chem.* 206 (1986) 69.
- [16] T. Huber, O. Pecina, W. Schmickler, *J. Electroanal. Chem.* 467 (1999) 203.
- [17] S. Frank, W. Schmickler, *J. Electroanal. Chem.* 483 (2000) 18.
- [18] S. Frank, W. Schmickler, *J. Electroanal. Chem.* 500 (2001) 491.
- [19] L.I. Daikhin, A.A. Kornyshev, M. Urbakh, *J. Electroanal. Chem.* 500 (2001) 461.
- [20] L.I. Daikhin, A.A. Kornyshev, M. Urbakh, *Electrochim. Acta* 45 (1999) 685.
- [21] L.I. Daikhin, A.A. Kornyshev, M. Urbakh, *J. Electroanal. Chem.* 483 (2000) 68.
- [22] O. Pecina, J.P. Badiali, *J. Electroanal. Chem.* 475 (1999) 46.
- [23] C.M. Pereira, F. Silva, M.J. Sousa, K. Kontturi, L. Murtomaki, *J. Electroanal. Chem.* 509 (2001) 148.
- [24] I. Benjamin, *Ann. Rev. Phys. Chem.* 48 (1997) 407.
- [25] I. Benjamin, *Science* 261 (1993) 1558.
- [26] Z. Samec, A. Lhotsky, H. Janchenova, V. Marecek, *J. Electroanal. Chem.* 483 (2000) 47.
- [27] K. Schweighofer, I. Benjamin, *J. Chem. Phys.* 112 (2000) 1474.